

# The effects of SiC<sub>p</sub> addition on the z-value and mechanical properties of $\beta$ -Sialon–SiC<sub>p</sub> refractories

Zhaohui HUANG, Juntong HUANG, Minghao FANG,<sup>†</sup> Saifang HUANG,  
Yan'gai LIU, Xiaoxian WU and Jingzhou YANG

School of Materials Science and Technology, China University of Geosciences (Beijing), Beijing 100083, P.R. China

The effects of SiC<sub>p</sub> addition on the z-value, microstructure and mechanical properties of  $\beta$ -Si<sub>6-z</sub>Al<sub>z</sub>O<sub>8-z</sub>–SiC<sub>p</sub> were investigated. The results showed that z-value of  $\beta$ -Sialon decreased from 2.66 to 1.20 with the increase of SiC<sub>p</sub> addition, while the apparent porosity of  $\beta$ -Sialon–SiC<sub>p</sub> composites increased. The bending strength and compressive strength decreased due to the increase of the apparent porosity and the weak cohesion resulted from the thermal expansion coefficient mismatch between SiC<sub>p</sub> and  $\beta$ -Sialon matrix. Moreover, a linear regression model used to identify the relationship between the content of SiC and z value of  $\beta$ -Sialon is fitted.

©2012 The Ceramic Society of Japan. All rights reserved.

Key-words :  $\beta$ -Sialon–SiC<sub>p</sub>, z-Value, Microstructure, Mechanical properties, Refractories

[Received March 7, 2012; Accepted May 8, 2012]

## 1. Introduction

$\beta$ -Sialon–SiC refractories have been widely used especially as blast furnace refractories, which is a critical and dominative factor for the quality of iron smelting and the lifespan of blast furnace,<sup>1)–3)</sup> due to their better alkali resistance, abrasion resistance and thermal shock resistance than high-alumina and corundum bricks, and better oxidation resistance and higher strength properties than carbon products.

Up to now, owning excellent properties, Sialon ceramics,<sup>4),5)</sup> Sialon crystals<sup>6),7)</sup> and Sialon-based composites<sup>8)–10)</sup> have attracted considerable attention as a kind of promising material for various applications. As to Sialon-based refractories, lots of studies have been performed and mainly concentrated on the effects of SiC contents and sintering additives (such as Y<sub>2</sub>O<sub>3</sub> and rare-earth oxides RE<sub>2</sub>O<sub>3</sub>) on preparation, microstructure and mechanical properties of  $\beta$ -Sialon–SiC refractories.<sup>11)–16)</sup> In addition, the effects of z value of  $\beta$ -Sialon (general formula of Si<sub>6-z</sub>Al<sub>z</sub>O<sub>8-z</sub>,<sup>17)</sup> where z-value reflects the substitution extent of Si, N atoms by Al, O atoms) on properties of  $\beta$ -Sialon–SiC refractories have been investigated as well.<sup>18)</sup> It has been revealed that the strength of materials at ambient temperature as well as high temperature were both found to be the best when z value is 2, and with the increase of z value, the thermal shock resistance of materials was improved, but alkali and slag resistance was decreased. Almost previous studies show that the formation of  $\beta$ -Sialon using Si<sub>3</sub>N<sub>4</sub>, AlN, Al<sub>2</sub>O<sub>3</sub> and RE<sub>2</sub>O<sub>3</sub> as starting materials is via a dissolution–precipitation mechanism.<sup>19)–21)</sup> The mechanism can be described as follows: initially, the SiO<sub>2</sub> presenting on the surface of Si<sub>3</sub>N<sub>4</sub> particles reacts with Al<sub>2</sub>O<sub>3</sub> and RE<sub>2</sub>O<sub>3</sub> forming a eutectic liquid of Al<sub>2</sub>O<sub>3</sub>–SiO<sub>2</sub>–RE<sub>2</sub>O<sub>3</sub> system, and then AlN dissolves gradually into the liquid with the increase of temperature; finally, the eutectic liquid can be absorbed partly into Si<sub>3</sub>N<sub>4</sub> thereby precipitating  $\beta$ -Sialon. It's well-known that there is a thin SiO<sub>2</sub> film on the surface of SiC particle, which also can be involved in the liquid reaction of

$\beta$ -Sialon during the sintering process of  $\beta$ -Sialon–SiC.<sup>14),15),22)</sup> From those researches, we can conclude that the adding SiC<sub>p</sub> should affect the z value of  $\beta$ -Sialon. However, there is little literature reporting the effect of SiC<sub>p</sub> addition on z value of  $\beta$ -Sialon.

In this paper,  $\beta$ -Sialon–SiC refractories were prepared with the powders of Si, Si<sub>3</sub>N<sub>4</sub>, AlN, Al<sub>2</sub>O<sub>3</sub> and SiC particles as starting materials and Y<sub>2</sub>O<sub>3</sub> as sintering additive which had been successfully used in the preparation of Si<sub>3</sub>N<sub>4</sub>, SiC and Sialon materials.<sup>13)–15)</sup> The effects of SiC addition on z-value of  $\beta$ -Sialon as well as microstructure and mechanical properties of  $\beta$ -Sialon–SiC refractories prepared by in-situ nitridation reaction were discussed. The present work has a certain signification for designing  $\beta$ -Sialon–SiC refractories.

## 2. Experimental procedures

Si powder (99 wt %, Beijing Dadi Zelin Silicon Co., Ltd., China), Si<sub>3</sub>N<sub>4</sub> powder (99.7 wt %, D<sub>50</sub> = 0.7  $\mu$ m;  $\alpha$ -phase >93.8 wt %, Shanghai Anseml Fine Ceramic Co., Ltd., China), AlN powder (98 wt %, D<sub>50</sub> = 0.5  $\mu$ m, Advanced Technology & Materials Co., Ltd., China), Al<sub>2</sub>O<sub>3</sub> powder (99.5 wt %, grain size <0.5  $\mu$ m, Beijing F&F Chemical Industrial Co., Ltd., China), SiC particles (98 wt %, 1.5 wt % O, Land Silicon Carbide Co., Ltd., China) as raw materials and Y<sub>2</sub>O<sub>3</sub> powder (99.99 wt %, General Research Institute Nonferrous Metals, China) as sintering additive were used to prepare the  $\beta$ -Sialon/SiC refractories. The gradation of SiC particles was: 15 wt % 44  $\mu$ m, 25 wt % 63  $\mu$ m, 45 wt % 160  $\mu$ m and 15 wt % 325  $\mu$ m.

The match ratio of Si, Si<sub>3</sub>N<sub>4</sub>, AlN and Al<sub>2</sub>O<sub>3</sub> powders in the starting materials was designed to obtain  $\beta$ -Si<sub>6-z</sub>Al<sub>z</sub>O<sub>8-z</sub> with z = 2 according to the Ref. 18). Si powder is not only translated into nitride reinforcement, but also plays the plastic role in shaping and sintering.<sup>23)</sup> The mol ratio of Si/Si<sub>3</sub>N<sub>4</sub> was 3, and 2 wt % Y<sub>2</sub>O<sub>3</sub> powder was extra-added. The composition of the samples investigated in this work is listed in Table 1. The extra oxygen contents presented in the nitrides were taken into account.

The mixtures of Si, Si<sub>3</sub>N<sub>4</sub>, AlN and Al<sub>2</sub>O<sub>3</sub> powders were milled with agate media in water-free ethanol for 6 h and

<sup>†</sup> Corresponding author: M. H. Fang; E-mail: fmh@cugb.edu.cn

Table 1. Composition of the samples

| Samples | Full Composition (wt %)  |                                |       |                                |       |   |
|---------|--|--------------------------------|-------|--------------------------------|-------|---|
|         | Composition of Si <sub>4</sub> Al <sub>2</sub> O <sub>2</sub> N <sub>6</sub> |                                |       |                                | SiC   | Y <sub>2</sub> O <sub>3</sub><br>(additional) |
|         | Si   | Si <sub>3</sub> N <sub>4</sub> | AlN   | Al <sub>2</sub> O <sub>3</sub> |       |   |
| S1      | 22.89  | 38.15                          | 11.17 | 27.79                          | 0.00  | 2.00  |
| S2      | 19.46  | 32.43                          | 9.49  | 23.62                          | 15.00 | 2.00  |
| S3      | 16.02  | 26.71                          | 7.82  | 19.45                          | 30.00 | 2.00  |
| S4      | 12.59  | 20.98                          | 6.14  | 15.28                          | 45.00 | 2.00  |
| S5      | 9.15   | 15.26                          | 4.47  | 11.12                          | 60.00 | 2.00  |

subsequently dried at 70°C for 24 h, then the mixtures were mixed with different amount of SiC particles (0, 15, 30, 45 and 60 wt %) and additional Y<sub>2</sub>O<sub>3</sub> powder in a fast ball mill with alumina grinding balls for 10 min. The final mixtures (designated as S1, S2, S3, S4 and S5, respectively) were uniaxial pressed into a shape of 6 mm × 6 mm × 40 mm, and cold isostatic pressed at 200 MPa. The samples (S1–S5) were placed in the graphite crucible and buried in pure BN powder, then sintered by in-situ nitridation reaction in flowing N<sub>2</sub> atmosphere (99.999 wt % purity) in a multi-functional furnace at 1600°C for 3 h. To ensure that silicon could be well nitrided thereby developing suitable microstructure, the heating process included four temperature holding stages: the samples were heated up from ambient temperature to 1150°C with a rate of 15°C/min holding for 1 h under 0.12 MPa of nitrogen pressure, and raised to 1280 and 1430°C with a rate of 10°C/min holding for 1 h under 0.9 MPa of nitrogen pressure, respectively, then heated to 1600°C from 1430°C with a rate of 10°C/min and finally sintered at this temperature for 3 h with a nitrogen pressure of 0.9 MPa.

The density and apparent porosity of the sintered samples were investigated by the Archimedes' method. The bending strength of the samples was measured by a three-point bending test with a 30 mm span at a crosshead speed of 0.5 mm/min at room temperature. The compressive strength of the samples was tested by exerting an axial compression. Phase identification was carried out by X-ray diffraction (XRD) using a XD-3 XRD equipment (Purkinje General, Cu K $\alpha$  radiation,  $\lambda = 1.5406 \text{ \AA}$ ). The lattice parameters of  $\beta$ -Sialon were calculated by the following equation:

$$d_{hkl} = \frac{a}{\sqrt{\frac{4}{3}(h^2 + hk + k^2) + \left(\frac{a}{c}\right)^2 \cdot l^2}} \quad (1)$$

where  $a$  and  $c$  is the unit lattice parameters of the final  $\beta$ -Sialon,  $d_{hkl}$  is the space distance between reflection planes ( $hkl$ ). Parameters  $a$  and  $c$  were calculated using the (200), (101) and (210) reflections of  $\beta$ -Sialon. The  $z$  value of  $\beta$ -Sialon phase in materials was obtained from the average values of  $z_a$  and  $z_c$  calculated from the following equations:<sup>24)</sup>

$$a = 7.603 + 0.0296z \text{ \AA} \quad (2a)$$

$$c = 2.907 + 0.0255z \text{ \AA} \quad (2b)$$

The microstructure of the samples was observed by scanning electron microscopy (SEM; JSM-6460, Japan) with an energy dispersive spectroscopy detector (EDS; INCAX-Sigh, Oxford, UK).

### 3. Results

#### 3.1 XRD analysis

Figure 1 shows the XRD patterns of the samples sintered in nitrogen atmosphere at the temperature of 1600°C holding for

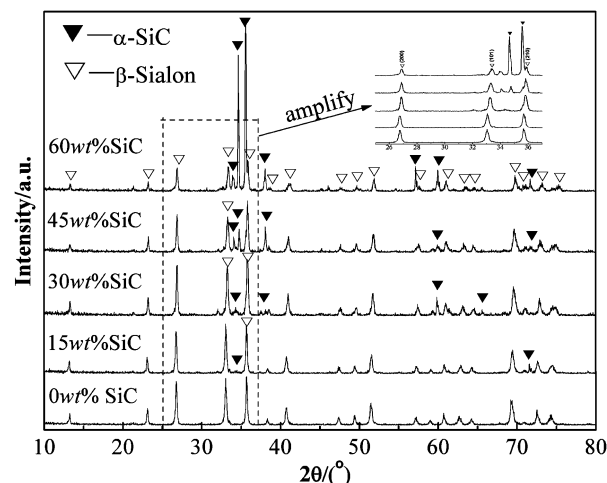


Fig. 1. XRD patterns of samples sintered at 1600°C for 3 h by in situ nitridation reaction.

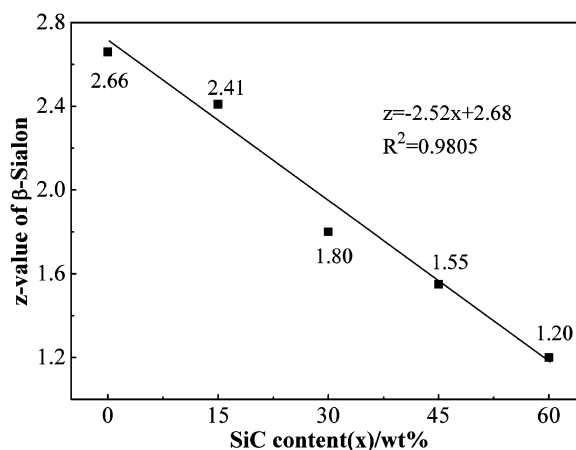


Fig. 2. Effect of the SiC addition on the  $z$  value of  $\beta$ -Sialon.

3 h. It is obvious that  $\alpha$ -SiC and  $\beta$ -Sialon synthesized by in-situ nitridation reaction were presented in the samples after the high-temperature reaction. From the partial amplified XRD patterns shown in the inset of Fig. 1, it can be seen that the positions of diffraction peaks of  $\beta$ -Sialon phase were shifted to the high-angle direction with the increase of SiC<sub>p</sub> content. According to the Eqs. (1) and (2), the  $z$  values of  $\beta$ -Sialon calculated from the XRD pattern are shown in Fig. 2. It is revealed that the  $z$  value of  $\beta$ -Sialon decreased from 2.66 to 1.20 with the increase of weight percentage ( $x$ ) of SiC<sub>p</sub> in the sample.

#### 3.2 SEM analysis

SEM micrographs of fracture samples with different addition of SiC sintered at 1600°C for 3 h by in-situ nitridation reaction are shown in Fig. 3. It clearly indicates that sample S1 with a few pores was well sintered [Fig. 3(a)]. The SiC particle was closely wrapped by  $\beta$ -Sialon matrix in sample S2 with 15 wt % SiC<sub>p</sub> [Fig. 3(b)], in which there were numbers of elongated  $\beta$ -Sialon with high aspect ratios. With the increase of SiC addition, more voids between SiC particles and  $\beta$ -Sialon matrix were present in the samples as shown in Figs. 3(c)–3(e). Moreover, we also observed the surfaces of the SiC particles in the  $\beta$ -Sialon-SiC<sub>p</sub> composites refractories, shown in the Fig. 4. The dense SiC particle has the surfaces with smooth areas and rough areas, where

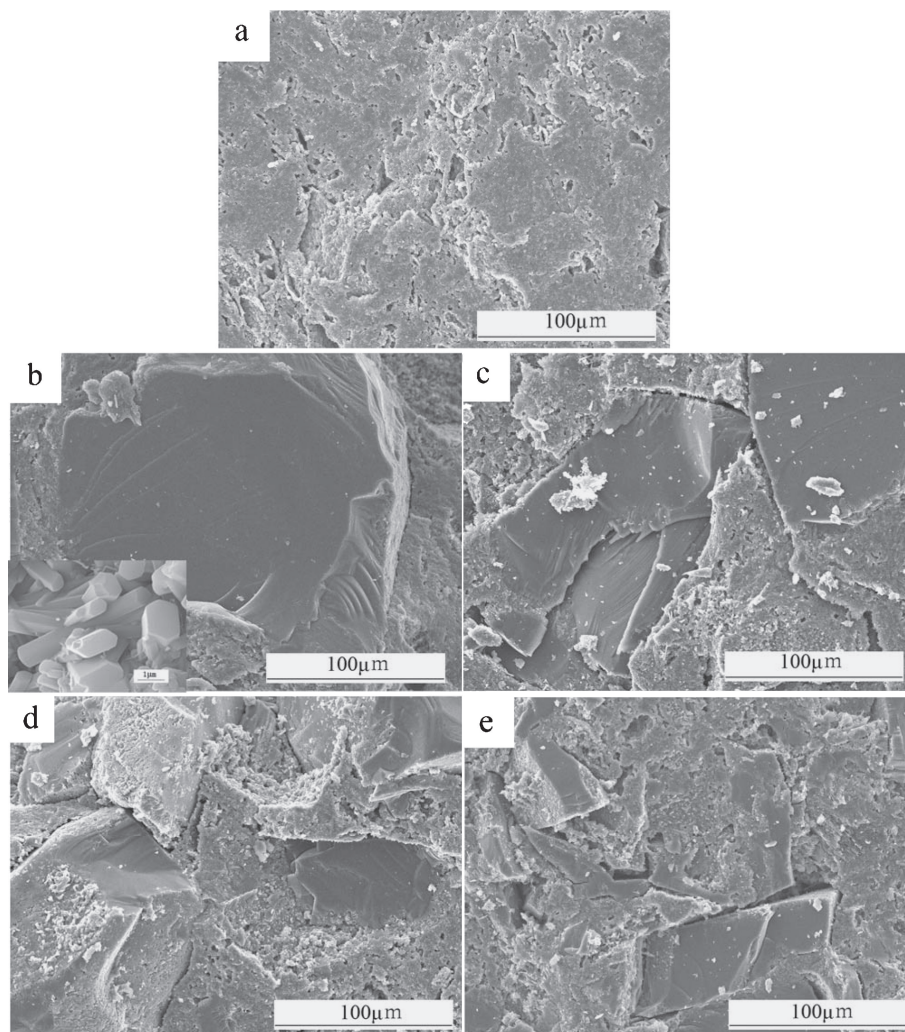


Fig. 3. Fracture surface microstructure of samples with different SiC contents sintered at 1600°C for 3 h (a) 0 wt% SiC, (b) 15 wt% SiC, (c) 30 wt% SiC, (d) 45 wt% SiC, (e) 60 wt% SiC.

besides Si and C elements, signals of Al, O and N elements can also be found in the EDS patterns [Figs. 4(c) and 4(d)].

### 3.3 Mechanical properties of $\beta$ -Sialon-SiC<sub>p</sub> refractories

**Figure 5** shows the apparent porosity and bulk density of  $\beta$ -Sialon-SiC<sub>p</sub> refractories as function of the SiC<sub>p</sub> addition. It is indicated that the sample S2 with 15 wt% SiC<sub>p</sub> had the highest bulk density of 2.86 g·cm<sup>-3</sup> and the lowest apparent porosity of 1.59% among the six samples. With the increase of SiC<sub>p</sub> addition, the apparent porosity of  $\beta$ -Sialon-SiC<sub>p</sub> refractory gradually increased, while the bulk density decreased.

The results of bending strength and compressive strength of the sintering samples as function of SiC<sub>p</sub> additions are shown in **Fig. 6**. It is obvious that, with the increase of SiC<sub>p</sub> content, the bending strength and compressive strength of the sintered samples decreased from 228 to 189 MPa and from 1080 to 428 MPa, respectively.

## 4. Discussion

### 4.1 Effect of SiC<sub>p</sub> addition on $z$ value of $\beta$ -Sialon

The positions of diffraction peaks of  $\beta$ -Sialon phase were shifted to the high-angle direction with the increase of SiC<sub>p</sub>

content (inset in Fig. 1), which should be attributed to the changed interplanar spacing  $d$ . It is well known that  $z$ -value of  $\beta$ -Sialon reflects the substitution extent of Si, N atoms by Al, O atoms, and the average Al-N bond (1.87 Å), Al-O bond (1.75 Å) is longer than the Si-N bond (1.74 Å), which is related to the unit lattice parameters.<sup>25)</sup> According to the Eq. (1), the unit lattice parameters have relationship with the interplanar spacing. Thus, the substitution extent, in other word,  $z$  value effects the interplanar spacing  $d$  of  $\beta$ -Sialon. As is shown in Fig. 2, the  $z$  value of  $\beta$ -Sialon decreased from 2.66 to 1.20 with the increase of weight percentage ( $x$ ) of SiC<sub>p</sub> in the sample. Thereby, the interplanar spacing  $d$  decreased, consequently, resulting in the shift to the high-angle  $\theta$ , according to Bragg's equation  $2d \sin \theta = n\lambda$ .

The decreased  $z$  value of the synthesized  $\beta$ -Sialon with the increase of SiC<sub>p</sub> addition can be explained by the following analysis. It is normally recognized that there is a thin SiO<sub>2</sub> film on the surface of SiC particle.<sup>15),22)</sup> Such a SiO<sub>2</sub> film could be involved in the liquid reaction generating  $\beta$ -Sialon phase, which was indicated by the EDS results of SiC<sub>p</sub> layers (Fig. 4). From the EDS patterns, it can be seen that besides Si and C elements existed in the SiC particle itself, signals of Al, O and N elements can also be found in the patterns. The  $z$  value was associated with

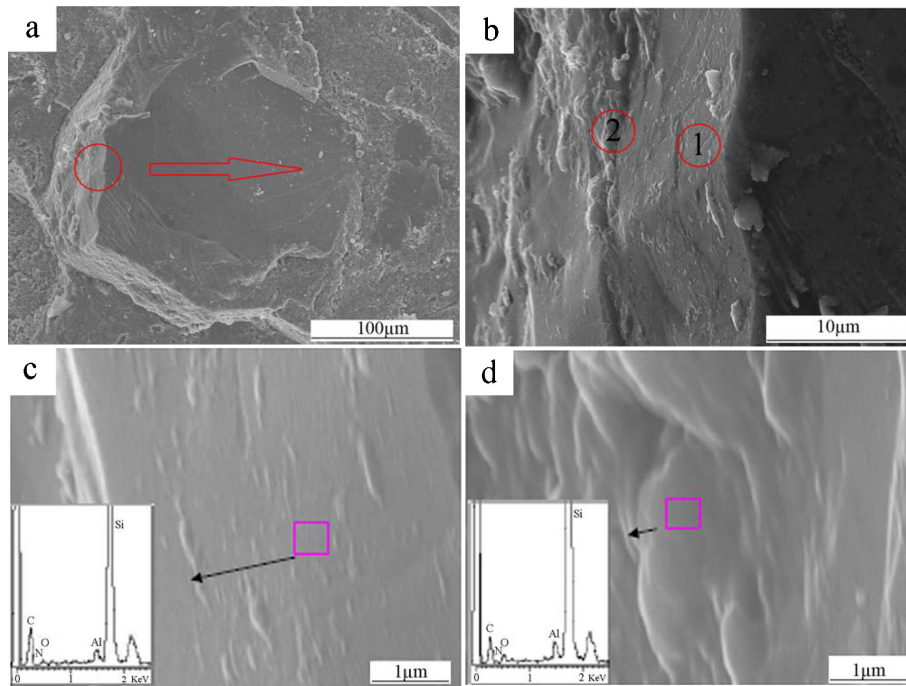


Fig. 4. (Color online) Morphologies of SiC surfaces in the sample with 15 wt% SiC sintered at 1600°C for 3 h (a) SiC particle, (b) Enlarged SEM image of surface of SiC particle in (a) as marked by the circle, (c) and (d) is zone 1 and zone 2 of (b) with the insert EDS pattern, respectively.

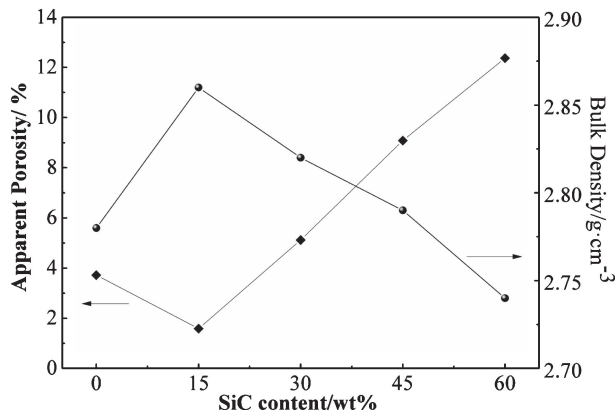


Fig. 5. Effect of the SiC addition on the apparent porosity and bulk density of  $\beta$ -Sialon-SiC composites.

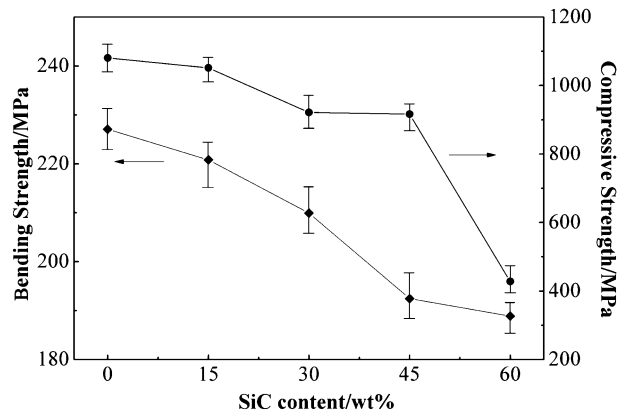
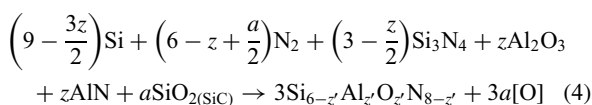
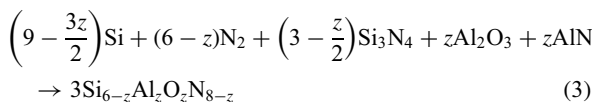


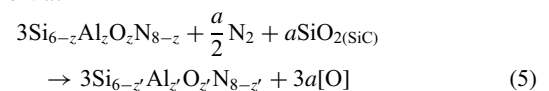
Fig. 6. Effect of the SiC addition on the bending strength and compressive strength of  $\beta$ -Sialon-SiC composites.

total content of SiO<sub>2</sub> existed in the samples, while the content of SiO<sub>2</sub> was affiliated with the addition of SiC particles. The SiO<sub>2</sub> contents increased as the SiC<sub>p</sub> content increased, resulted in large amount of SiO<sub>2</sub> being involved in the liquid reaction of  $\beta$ -Sialon. It can be analyzed by the following reaction equations:



Equation (3) is the reaction equation of  $\beta$ -Sialon without SiO<sub>2(SiC)</sub>, i.e. the SiO<sub>2</sub> on the surface of SiC particles, where  $z$  is the value of  $\beta$ -Sialon in the sample without SiC particles. Equation (4) is the reaction equation of  $\beta$ -Sialon with SiO<sub>2(SiC)</sub>,

where  $z'$  is the real  $z$  value of  $\beta$ -Sialon after absorbed the SiO<sub>2</sub> composition, and  $a$  is a coefficient in direct ratio to the content of SiO<sub>2(SiC)</sub>. The Eq. (4) can be abstractly understood to be that SiO<sub>2</sub> on the surface of SiC particles participated in the reaction of Eq. (3), which can be concisely expressed to be Eq. (5). Thus, the Eq. (6) can be easily derived according to the mass conservation of silicon element according to the Eq. (5), which reflects that  $z'$  value of  $\beta$ -Sialon decreased with the increase of coefficient  $a$ .



$$z' = z - \frac{a}{3} \quad (6)$$

The tendency of  $z$  value of  $\beta$ -Sialon in  $\beta$ -Sialon/SiC<sub>p</sub> composites against the SiC<sub>p</sub> addition shown in Fig. 2 was consistent with the anti-linear relationship between  $z'$  value of  $\beta$ -Sialon



and coefficient  $a$ . A fitted linear regression model can be used to identify the relationship between the independent variable  $x$  (the content of SiC) and the dependent variable  $z$  ( $z$  value of  $\beta$ -Sialon) by the following equation with a reliability value of  $R^2 = 0.9805$ :

$$z = -2.52x + 2.68 \quad (7)$$

The results strongly prove that the effect of SiC<sub>p</sub> additions on the  $z$  value of  $\beta$ -Sialon must be taken into account during the design process of  $\beta$ -Sialon/SiC<sub>p</sub> refractories, if an accurate  $z$  value is required.

## 4.2 Effect of SiC<sub>p</sub> addition on the microstructure, bulk density and apparent porosity of $\beta$ -Sialon-SiC<sub>p</sub> refractories

When the sintering temperature is 1600°C, pure SiC is hardly sintered, but, Sialon bonding phase can change the sintering property of SiC. The bulk density of Sialon-SiC composites is detected by the sintering of green body. The increasing of bulk density means more compact sintered materials, better bond between different components. Holes in the materials are continuously closed during the sintering process so that the apparent porosity decreased, however, the variation of bulk density showed the opposite trend, and vice versa. Figure 5 shows the relationship between the bulk density and apparent porosity just agreed with that variation law.

It is quite easily seen from SEM microstructure of the samples (Fig. 3) that more voids between SiC particles and  $\beta$ -Sialon matrix with the increase of SiC addition. SiC<sub>p</sub> could be closely wrapped by enough Sialon matrix when the SiC<sub>p</sub> content was low. In contrast, the SiC particles could not be fully packed by Sialon fine grains thereby generating pores among adjacent SiC particles with the increase of SiC<sub>p</sub> addition. Such bonding station between SiC<sub>p</sub> and Sialon resulted in the increase of the apparent porosity and the decrease of the bulk density with the increase of SiC<sub>p</sub> addition, which had similar phenomenon with other works established in different systems.<sup>12),26)</sup>

## 4.3 Effect of SiC<sub>p</sub> addition on the mechanical properties of $\beta$ -Sialon-SiC<sub>p</sub> refractories

With the increase of SiC<sub>p</sub> addition, the bending strength and compressive strength of the sintered samples decreased (Fig. 6). Though the  $z$ -value of  $\beta$ -Sialon partly affect the mechanical properties of  $\beta$ -Sialon-SiC refractories according to the Ref. 18), where the content of SiC is constant. In this work, we investigated emphatically the effect of SiC addition on  $z$ -value of  $\beta$ -Sialon in order to illustrate that the effect of SiC addition on  $z$ -value of  $\beta$ -Sialon should be taken into account when designing  $\beta$ -Sialon-SiC refractories. Herein, the effect of SiC<sub>p</sub> addition which is variable on the mechanical properties of  $\beta$ -Sialon-SiC<sub>p</sub> refractories was also discussed. In this paper, relative to the effect of  $z$ -value, the porosity and the interface cohesion between SiC<sub>p</sub> and  $\beta$ -Sialon should be the main responsible for the mechanical properties.

As is well-known, the strength-porosity dependence can be approximated by the following exponential equation:<sup>27)</sup>

$$\sigma = \sigma_0 \cdot \exp(-np) \quad (8)$$

Where  $\sigma_0$  is the strength of a nonporous structure,  $\sigma$  is the strength of the porous structure at a porosity  $p$ , and  $n$  is a constant.

Generally, the mechanical strength of inorganic non-metallic materials decreases with the increase of the porosity. In this work, the strength-porosity relationship of the sintering samples

added with SiC<sub>p</sub> (S2-S5) could comply with it. In comparison, the bending strength of the sample with 15 wt % SiC<sub>p</sub> (S2) was no higher than pure  $\beta$ -Sialon ceramic (S1), even though sample S2 had a lower apparent porosity. Thus, in this case, the decrease of mechanical properties is attributed to the weak cohesion resulting from thermal expansion coefficient mismatch between SiC ( $\alpha = 4.3 \times 10^{-6} \text{ K}^{-1}$ )<sup>14)</sup> and  $\beta$ -Sialon matrix ( $\alpha = 3.2 \times 10^{-6} \text{ K}^{-1}$ ).<sup>28)</sup> The increase of the SiC<sub>p</sub> content in samples S2-S5 resulted in lower densification of materials. The reduction of the area on which the stress loaded caused the decrease of compressive strength. Though the mechanical properties of the  $\beta$ -Sialon-SiC<sub>p</sub> composites decreased, they could still satisfy the requirements of refractories in the blast furnace.

## 5. Conclusions

$\beta$ -Sialon-SiC<sub>p</sub> refractories were prepared by in-situ nitridation reaction at 1600°C for 3 h using a mixture of Si, Si<sub>3</sub>N<sub>4</sub>, AlN, Al<sub>2</sub>O<sub>3</sub> and Y<sub>2</sub>O<sub>3</sub> powders with different amount of SiC particles. The results showed that, with the increase of SiC<sub>p</sub> addition (from 0 to 60 wt %), the  $z$ -value of the  $\beta$ -Sialon in the  $\beta$ -Sialon-SiC<sub>p</sub> composites decreased from 2.66 to 1.20. Meanwhile, the bending strength and compressive strength of the composites exhibited a certain decrease from 228 to 189 MPa and from 1080 to 428 MPa, respectively. Moreover,  $\beta$ -Sialon-SiC<sub>p</sub> refractories had the bulk density of 2.86 g·cm<sup>-3</sup> and the apparent porosity of 1.59% with the optimized SiC<sub>p</sub> addition of 15 wt %. The relevant mechanical properties of the  $\beta$ -Sialon-SiC<sub>p</sub> composites with SiC<sub>p</sub> addition of 0-60 wt % could match the corresponding requires of blast-furnace refractories.

**Acknowledgments** This work was financially supported by National Natural Science Foundation of China (Grant Nos. 50972134 and 51032007), New Star Technology Plan of Beijing (Grant No. 2007A080), and the Fundamental Research Funds for Central Universities (Grant Nos. 2009PY09 and 2009PY10).

## References

- 1) D. A. Gunn, *J. Eur. Ceram. Soc.*, **11**, 35-41 (1993).
- 2) W. Sui, S. Luan and R. Song, *Key Eng. Mater.*, **336-338**, 1498-1500 (2007).
- 3) H. Zhang, B. Han and Z. Liu, *Mater. Res. Bull.*, **41**, 1681-1689 (2006).
- 4) Z. J. Shen, Z. Zhao, H. Peng and M. Nygren, *Nature*, **417**, 266-269 (2002).
- 5) Z. J. Shen, H. Peng, P. Pettersson and M. Nygren, *J. Am. Ceram. Soc.*, **85**, 2876-2878 (2002).
- 6) S. F. Huang, Z. H. Huang, M. H. Fang, Y. G. Liu, J. T. Huang and J. Z. Yang, *Cryst. Growth Des.*, **10**, 2439-2442 (2010).
- 7) S. F. Huang, Z. H. Huang, Y. G. Liu and M. H. Fang, *Dalton Trans.*, **40**, 1261-1266 (2011).
- 8) R. Shuba and I. W. Chen, *J. Am. Ceram. Soc.*, **89**, 2147-2153 (2006).
- 9) J. Z. Yang, Z. H. Huang, M. H. Fang, Y. G. Liu, J. T. Huang and J. H. Hu, *Scr. Mater.*, **61**, 632-635 (2009).
- 10) J. Z. Yang, Z. H. Huang, X. Z. Hu, M. H. Fang, Y. G. Liu and J. T. Huang, *Mater. Sci. Eng., A*, **528**, 2196-2199 (2011).
- 11) S. Dong, D. Jiang, S. Tan and J. Guo, *Mater. Lett.*, **29**, 259-263 (1996).
- 12) Q. Liu, L. Gao, D. Yan and D. P. Thompson, *Mater. Sci. Eng., A*, **269**, 1-7 (1999).
- 13) C. Ke, J. J. Edrees and A. Hendry, *J. Eur. Ceram. Soc.*, **19**, 2165-2172 (1999).
- 14) M. Lin, G. Chena, Y. Yang, D. Jiang and J. Shi, *Mater. Sci. Eng., A*, **433**, 329-333 (2006).

- 15) A. A. Nourbakhsh, F. Golestani-Fard and H. R. Rezaie, *J. Eur. Ceram. Soc.*, **26**, 1737–1741 (2006).
- 16) J. Moffatt and L. Edwards, *Int. J. Fatigue*, **30**, 1289–1297 (2008).
- 17) K. Aoyagi, T. Hiraki, R. Sivakumar, T. Watanabe and T. Akiyama, *J. Am. Ceram. Soc.*, **90**, 626–628 (2007).
- 18) T. Hirota, *Taikabutsu Oversea*, **47**, 211–219 (1995).
- 19) S. L. Hwang and I. Chen, *J. Am. Ceram. Soc.*, **77**, 165–171 (1994).
- 20) T. Ekstrom and M. Nygren, *J. Am. Ceram. Soc.*, **75**, 259–276 (1992).
- 21) H. Miyazaki, M. I. Jones and K. Hirao, *Mater. Lett.*, **59**, 44–47 (2005).
- 22) P. Tartaj, M. Reece and S. M. Jose, *J. Am. Ceram. Soc.*, **81**, 389–394 (1998).
- 23) L. Rangaraj, C. Divakar and V. Jayaram, *Key Eng. Mater.*, **395**, 69–88 (2009).
- 24) J. V. C. Souza, C. Santos, C. A. Kelly and O. M. M. Silva, *Int. J. Refract. Met. Hard Mater.*, **25**, 77–81 (2007).
- 25) Z. J. Shen and M. Nygren, *J. Eur. Ceram. Soc.*, **17**, 1639–1645 (1997).
- 26) C. Santos, C. A. Kelly, S. Ribeiro, K. Strecker, J. V. C. Souza and O. M. M. Silva, *J. Mater. Process. Technol.*, **189**, 138–142 (2007).
- 27) K. Ishizaki, S. Komarneni and M. Nanko, “Porous Materials: Process Technology and Applications,” Kluwer Academic Publishers, Dordrecht, the Netherlands (1998).
- 28) D. Baril, S. P. Tremblay and M. Fiset, *J. Mater. Sci.*, **28**, 5486–5494 (1993).